Co-ordination Tendencies of Two Novel Compartmental Oxa-aza Macrobicycles. Crystal Structure of a $Cu^{II}(H_2O)$ Inclusion Complex†

Carla Bazzicalupi, Andrea Bencini,* Antonio Bianchi,* Vieri Fusi, Claudia Giorgi, Piero Paoletti* and Barbara Valtancoli
Department of Chemistry, University of Florence, Via Maragliano 75/77, 50144 Florence, Italy

---

The two novel aza-oxa cryptands 16,21-dimethyl-4,7,10-trioxa-1,13,16,21-tetraazabicyclo[11.5.5]-tricosane (L^1) and 19,24-dimethyl-4,7,10,13-tetraoxa-1,16,19,24-tetraazabicyclo[14.5.5]hexacosane (L^2) can bind in aqueous solution Li^+ or Na^+ as well as Cu^{2+}, Zn^{2+} or Cd^{2+}. The co-ordination features of the above receptors have been studied in aqueous solution by potentiometric (298.1 or 318.1 K, I = 0.15 mol dm^{-3}) and spectroscopic (^1H and ^{13}C NMR and UV/VIS) techniques. In the case of Cu^{2+}, Zn^{2+} and Cd^{2+} both the thermodynamic and spectroscopic data are in accord with the metal centres co-ordinated by the tetraaza moiety of the receptor. The co-ordination sphere is completed by binding water molecules or an oxygen of the polyoxa chain. The crystal structures of $[CuL^1][ClO_4]_2\cdot 0.4MeOH$ and $[CuL^2(H_2O)][ClO_4]_2$ have been determined. In the former the metal ion is bound by the four nitrogens and by an oxygen donor of the ligand, giving rise to a rather distorted square-pyramidal co-ordination geometry. In the latter the four nitrogen atoms of the ligand are again involved in the co-ordination to the metal ion; the resulting geometry is fairly distorted square-pyramidal, with the fifth co-ordinative position occupied by the oxygen of a water molecule. The $Cu(H_2O)$ unit is encapsulated inside the molecular cavity, stabilized by hydrogen bonds between the water molecule and the four oxygens of the receptor. Consequently, the Cu–O distance is remarkably short (2.09 Å). This complex can lose the co-ordinated water molecule both in non-aqueous solution and in the solid state. The acidic dissociation of the Cu^{2+} complexes has also been studied in 1 mol dm^{-3} $HClO_4$ at different temperatures and the rate constants and activation parameters determined.

In the last last few years there has been considerable interest in the development of new oxa-aza macrobicyclic receptors.[1] Macropolycyclic molecules containing appropriate binding sites and cavities of suitable size and shape may be designed to form selective inclusion complexes. In fact, the molecular topology of the host molecule can be synthetically modulated in order to bind many different chemical species. To this purpose, oxa-aza macropolycyclic receptors able to bind different kinds of substrates, such as inorganic or organic cations,[2–7] anionic species,[5–8] and neutral molecules[9] have been studied to elaborate their use as selective recognizers, molecular carriers and catalysts.

In a recent paper we reported the synthesis and basicity properties of two new oxa-aza macrobicyclic receptors, 16,21-dimethyl-4,7,10-trioxa-1,13,16,21-tetraazabicyclo[11.5.5]tricosane (L^1) and 19,24-dimethyl-4,7,10,13-tetraoxa-1,16,19,24-tetraazabicyclo[14.5.5]hexacosane (L^2), which display two different binding subunits (one N_4 and one O_3 or O_4 framework).[10] The diprotonated form of such ligands can bind a water molecule into the macrobicyclic cavity, held by an arrangement of hydrogen bonds involving the protonated nitrogens and the oxygen atoms of the macrocycle. The resulting 'water cryptate' is characterized by high thermodynamic stability.

In order to obtain further information on the co-ordination features of these receptors, we have analysed their binding ability toward metal cations.

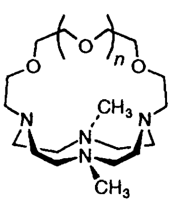

L^1 n = 1
L^2 n = 2

Results and Discussion

Description of the Structures.—$[CuL^1][ClO_4]_2\cdot 0.4MeOH$. The molecular structure consists of discrete $[CuL^1]^{2+}$ cations, perchlorate anions and lattice methanol molecules. ORTEP[11] drawings of the two independent cations A and B are shown in Fig. 1 together with the atom labelling. Bond lengths and angles for the co-ordination sphere of both metals are listed in Table 1.

The overall conformations of the two independent complexed cations are similar: the Cu^{2+} ions are five-co-ordinated by the four nitrogen atoms and an ethereal oxygen adjacent to the bridgehead nitrogen. The co-ordination geometries result in distorted square-pyramidal arrangements. The basal planes in both cases are determined by the nitrogen atoms, the deviations being in the range 0.03(2)–0.07(3) Å for A and 0.01(4) Å for all the nitrogens of B. The Cu–N bond distances are very similar in the two cations (see Table 1).

The atoms Cu(1) and Cu(2) are displaced 0.506(4) and 0.545(5) Å, respectively, from the least-squares basal planes towards the apex of the pyramid, occupied by O(3) and O(4) for A and B, respectively. The apical bond lengths are 2.37(2) Å for Cu(1)–O(3) and 2.24(3) Å for Cu(2)–O(4). The Cu(1)–O(3) bond forms an angle of 30.0(8)° with the normal to the basal

---

† *Supplementary data available:* see Instructions for Authors, *J. Chem. Soc., Dalton Trans.*, 1994, Issue 1, pp. xxiii–xxviii.

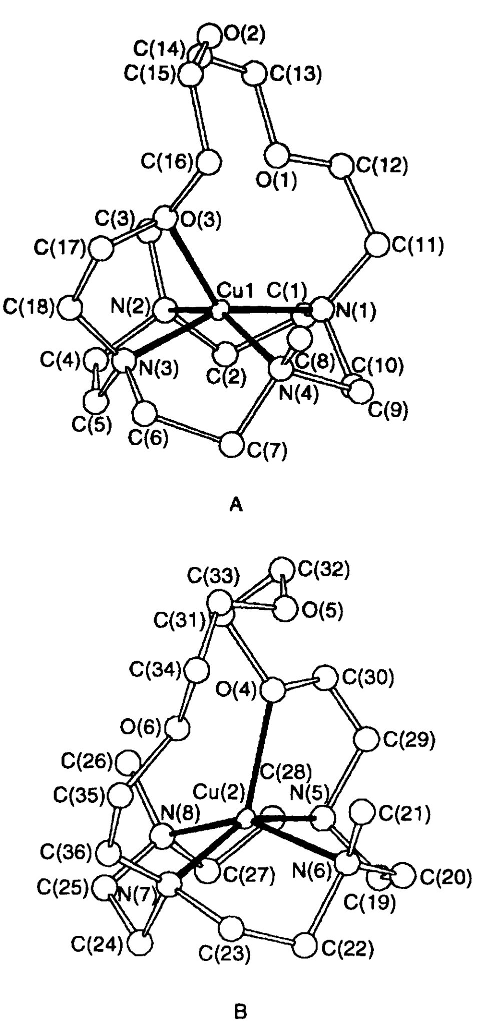

Fig. 1 ORTEP drawings of the $[CuL^1]^{2+}$ cations A and B. Thermal ellipsoids are at the 20% probability level

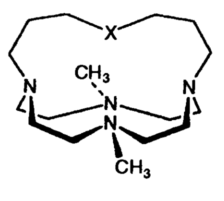

L^3 X = NH
L^4 X = O

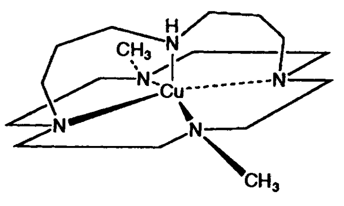

Table 1 Selected bond lengths (Å) and angles (°), with estimated standard deviations in parentheses, for $[CuL^1][ClO_4]_2\cdot0.4MeOH$

Cu(1)–N(1)	2.04(3)	Cu(2)–N(5)	2.01(2)
Cu(1)–N(2)	2.13(3)	Cu(2)–N(6)	2.21(3)
Cu(1)–N(3)	1.99(2)	Cu(2)–N(7)	2.12(4)
Cu(1)–N(4)	2.09(3)	Cu(2)–N(8)	1.99(3)
Cu(1)–O(3)	2.37(2)	Cu(2)–O(4)	2.24(3)
N(4)–Cu(1)–O(3)	95(1)	N(8)–Cu(2)–O(4)	104(1)
N(3)–Cu(1)–O(3)	75.4(8)	N(7)–Cu(2)–O(4)	132(1)
N(3)–Cu(1)–N(4)	88(1)	N(7)–Cu(2)–N(8)	85(1)
N(2)–Cu(1)–O(3)	112.2(9)	N(6)–Cu(2)–O(4)	102(1)
N(2)–Cu(1)–N(4)	149(1)	N(6)–Cu(2)–N(8)	150(1)
N(2)–Cu(1)–N(3)	87(1)	N(6)–Cu(2)–N(7)	88(1)
N(1)–Cu(1)–O(3)	131(1)	N(5)–Cu(2)–O(4)	80(1)
N(1)–Cu(1)–N(4)	85(1)	N(5)–Cu(2)–N(8)	85(1)
N(1)–Cu(1)–N(3)	153(1)	N(5)–Cu(2)–N(7)	149(1)
N(1)–Cu(1)–N(2)	86(1)	N(5)–Cu(2)–N(6)	85(1)

Table 2 Selected bond lengths (Å) and angles (°), with estimated standard deviations in parentheses, for $[CuL^2(H_2O)][ClO_4]_2$

Cu–O(5)	2.090(7)	Cu–N(3)	2.11(1)
Cu–N(1)	2.07(1)	Cu–N(4)	2.05(1)
Cu–N(2)	2.035(9)		
N(3)–Cu–N(4)	85.5(4)	N(1)–Cu–N(2)	85.8(4)
N(2)–Cu–N(4)	149.4(4)	O(5)–Cu–N(4)	100.4(4)
N(2)–Cu–N(3)	85.9(4)	O(5)–Cu–N(3)	104.5(4)
N(1)–Cu–N(4)	87.3(4)	O(5)–Cu–N(2)	110.2(4)
N(1)–Cu–N(3)	150.3(4)	O(5)–Cu–N(1)	105.1(4)

plane of A, while the corresponding value for Cu(2)–O(4) is 26.5(8)°.

The metal to plane distances are longer than those usually found for similar N_4XCu square-pyramidal complexes [12,13] and can be explained by considering that the four nitrogen atoms of the ligand belong to a small 12-membered macrocyclic ring. In fact, the Cu^{2+} complex of the pentaaza macrobicyclic ligand L^3,[14] which contains the same 12-membered ring, is characterized by a comparable metal–basal plane distance.

$[CuL^2(H_2O)][ClO_4]_2$. The structure consists of discrete $[CuL^2(H_2O)]^{2+}$ cations and perchlorate anions. An ORTEP [11] drawing of the complexed cation is shown in Fig. 2(*a*) and Table 2 reports the co-ordination bond lengths and angles.

The four nitrogen atoms of the ligand are involved in the co-ordination of the metal ion; the resulting geometry is fairly distorted square-pyramidal, with the fifth co-ordinative position occupied by the O(5) oxygen of a water molecule encapsulated inside the molecular cavity. The nitrogen atoms are almost coplanar [maximum deviation 0.002(11) Å for N(4)] and determine the basal plane of the pyramid. The Cu–N distances fall in the range 2.035(9)–2.11(1) Å.

Similarly to the Cu^{2+} complex of L^1, the metal ion is displaced by 0.537(1) Å from the mean plane determined by the four nitrogens, shifted towards the apical water molecule. The Cu–O(5) apical bond is approximately perpendicular to the basal plane, the angle with the normal being 4.9(3)°, and presents a remarkably short bond length [2.090(7) Å], comparable with the basal Cu–N bond lengths. This distance is shorter than those reported for several Cu^{2+} complexes with the same number and type of donor atoms and analogous co-ordination geometry (the apical bond lengths usually range from 2.20 to 2.89 Å).[12] This can be attributed to the inclusion of the $Cu(H_2O)$ unit into the macrocyclic cavity. The mean plane described by the four ethereal oxygen atoms and the N(1) and N(3) nitrogens [deviations from 0.155(9) Å for O(1) to 0.68(1) Å for N(3)] is almost perpendicular to the N_4 basal plane, forming a dihedral angle of 93.6(2)°. Each oxygen atom of the ligand has at least one electron pair pointing towards the cavity; therefore they are able to interact *via* hydrogen bonds with the water molecule encapsulated inside the ligand, the O(5)$\cdots$O distances being 2.88(1), 2.89(1), 2.93(1) and 2.75(1) Å for O(1), O(2), O(3) and O(4), respectively.

The crystal structure of the diprotonated species of L^2 shows a water molecule enclosed in the molecular cavity,[10] interacting *via* hydrogen bonds with both the protonated nitrogens and three oxygen atoms. The overall conformations of the ligand in both structures are very similar; the most significant difference is presented by the N(1)–C(9)–C(10)–O(1) torsion angle [−33(2)° in the present structure *vs.* 53.0° for $[H_2L^2(H_2O)]^{2+}$]. This angular value gives rise to a different orientation for the electronic pairs of O(1) in $[CuL^2(H_2O)]^{2+}$ with respect to $[H_2L^2(H_2O)]^{2+}$, where O(1) is not involved in hydrogen-bonding interactions with the enclosed water molecule. It is of interest that the water molecule occupies a similar position in both structures. In fact, the water molecule lies approximately on the normal to the N_4 mean plane and the distance of the

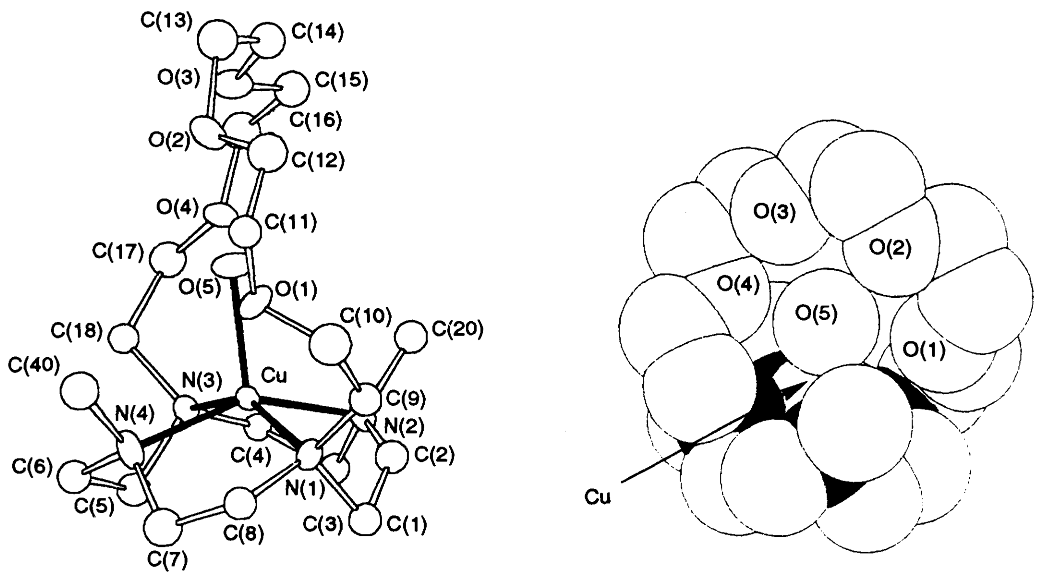

(a) (b)

Fig. 2 (*a*) ORTEP drawing (thermal ellipsoids are the 20% probability level) and (*b*) space filling representation (nitrogen atoms shown in black) of the $[CuL^2(H_2O)]^{2+}$ cation

Table 3 Logarithms of the formation constants of metal complexes of L^1 and L^2 in 0.15 mol dm^{-3} NMe_4ClO_4 aqueous solution at 318.1 ± 0.1 K

Reaction	Cu^{2+}	Zn^{2+}	Cd^{2+}
$M^{2+} + L^1 \rightleftharpoons [ML^1]^{2+}$	12.10(3)*	10.43(2)	11.33(3)
$[ML^1]^{2+} + OH^- \rightleftharpoons [ML^1(OH)]^+$	4.5(1)	4.5(1)	4.1(1)
$[ML^1(OH)]^+ + OH^- \rightleftharpoons [ML^1(OH)_2]$	—	4.0(1)	3.3(2)
$M^{2+} + L^2 \rightleftharpoons [ML^2]^{2+}$	14.34(3)	12.51(4)	12.04(2)
$[ML^2]^{2+} + OH^- \rightleftharpoons [ML^2(OH)]^+$	—	3.9(1)	3.1(1)
$[ML^2(OH)]^+ + OH^- \rightleftharpoons [ML^2(OH)_2]$	—	3.6(1)	3.4(1)

* Values in parentheses are standard deviations on the last significant figure.

oxygen atom from this plane is 2.620(8) Å for the $[CuL^2(H_2O)]^{2+}$ cation and 2.234 Å for $[H_2L^2(H_2O)]^{2+}$; this difference can be ascribed to the presence of the Cu^{2+} cation.

Solution Studies.—The reactions of Cu^{2+}, Zn^{2+} and Cd^{2+} with both L^1 and L^2 in aqueous solution are too slow at 298.1 K to determine confidently the stability constants of their complexes at this temperature, as already found for other polyaza cryptands.[15] For this reason, the determination of the equilibrium constants for the reactions of both ligands with the above metal ions have been carried out at 318.1 K in 0.15 mol dm^{-3} NMe_4ClO_4 aqueous solution. To this end, the protonation constants of the ligands have been determined in the same conditions. Their values [$\log K_1 = 10.66(1)$,† $\log K_2 = 8.08(3)$ for L^1 and $\log K_1 = 10.76(2)$, $\log K_2 = 8.34(3)$ for L^2] are in good agreement with those calculated from the protonation constants measured at 298.1 K.‡

The stability constants for the complexes formed by these receptors with Cu^{2+}, Zn^{2+} and Cd^{2+} are reported in Table 3. All the metal ions form $[ML]^{2+}$ complexes ($M = Cu^{2+}, Zn^{2+}, Cd^{2+}$; $L = L^1$ or L^2) with both ligands, but do not interact with protonated species of the macrobicycles. This behaviour can be ascribed to the full involvement of the tetraaza moiety in co-ordination to the metal ions,[16,§] as confirmed by the crystal structures of the $[CuL^1]^{2+}$ and $[CuL^2(H_2O)]^{2+}$ cations.

Cu^{2+} *Co-ordination*. The stability constants for the $[CuL]^{2+}$ ($L = L^1$ or L^2) species are considerably lower than those reported for monocyclic tetraazaalkanes.[1a,16] The presence of short ethylenic chains on the 12-membered tetraaza moiety makes this part of the overall molecular framework rather rigid. The two methyl groups in the *trans* position further contribute to the molecular crowding. These features, together with the polyoxa bridge that leads to a further stiffening of the backbone, can prevent the donor atoms from adapting themselves to the stereochemical requirements of the metal centres, thereby lowering the stability of the $[CuL]^{2+}$ complexes. Moreover, even the formation of large chelating rings containing the unbound oxygen atoms could contribute to such a decrease.[17]

As far as the $[CuL^2]^{2+}$ complex is concerned, it seems likely that the co-ordination sphere for the Cu^{2+} ion found in the solid state is also maintained in aqueous solution. The complex shows very similar electronic spectra in aqueous solution (a broad band with $\lambda_{max} = 625$ nm, $\varepsilon = 260$ dm^3 mol^{-1} cm^{-1}) and in the solid state ($\lambda_{max} = 630$ nm). Furthermore, a violet complex of stoichiometry $[CuL^2][ClO_4]_2$ can be obtained as a solid from non-aqueous media or synthesized by heating the solid $[CuL^2(H_2O)][ClO_4]_2$ at 80 °C. Its spectral features (a

---

† The basicity constants are relative to equilibrium $H_nL^{n+} + H^+ \rightleftharpoons H_{n+1}L^{(n+1)+}$, $n = 0$ or 1. The values in parentheses are the standard deviations on the last significant figure.

‡ $\log K_1 = 10.7(1)$, $\log K_2 = 7.9(1)$ for L^1 and $\log K_1 = 11.0(1)$, $\log K_2 = 8.2(1)$ for L^2 are obtained at 318.1 K by using the relation $\ln K_{318.1} - \ln K_{298.1} = \Delta H^\circ (1/298.1 - 1/318.1)/R$ where $K_{298.1}$ and ΔH° are respectively the protonation constants and enthalpies at 298.1 K (taken from ref. 10).

§ Most of the formation constants and relative ΔG° values reported in these references have been determined at 298 K. However, the ΔG° values calculated at 318.1 K using the Van't Hoff equation (where ΔH° is available) differ from those at 298 K by < 4 kJ mol^{-1}.

broad band with λ_{max} = 535 nm, ε = 380 dm^3 mol^{-1} cm^{-1} in methanol solution, λ_{max} = 550 nm in the solid state) are remarkably different from those presented by the $[CuL^2(H_2O)]^{2+}$ species. The compound $[CuL^2][ClO_4]_2$ is not stable on exposure to air at room temperature, and at < 80 °C, again takes up a water molecule. This confirms the high affinity for the $Cu-OH_2$ inclusion species. Similarly, the $[CuL^2(H_2O)]^{2+}$ species can be obtained by adding water to a methanol solution of $[CuL^2]^{2+}$. In other words, in water the Cu^{2+} ion is characterized by a co-ordination environment similar to that exhibited by the crystal structure of $[CuL^2(H_2O)][ClO_4]_2$ (see Fig. 2), while in organic media no water molecule is bound to the metal centre.

It is also of interest that, among the metal–ligand systems investigated, only $[CuL^2]^{2+}$ does not form hydroxo species (see Table 3), *i.e.*, the water molecule co-ordinated to the Cu^{2+} ion does not deprotonate, at least in the pH range considered.

Indeed, the $Cu-OH_2$ species exhibits a stereochemistry complementary with the binding sites of the ligand, as shown by the crystal structure of $[CuL^2(H_2O)][ClO_4]_2$ [Fig. 2(*b*)]. The metal ion is co-ordinated by the four nitrogen atoms of the macrocycle and is characterised by a fairly distorted square-pyramidal co-ordination environment with the O(5) oxygen of a water molecule in the apical position. This water molecule is lodged inside the tetraoxa moiety and interacts *via* hydrogen bonds with the four oxygen atoms of the receptor. The inclusion of the $Cu-OH_2$ unit into the macrocyclic cavity leads to a remarkably short Cu–O(5) bond length [2.090(7) Å], comparable with the basal Cu–N bond lengths. Such an array can represent a stable disposition from an energetic point of view, explaining the high affinity for the $Cu-OH_2$ inclusion species.

The ligand L^2 operates a dimensional recognition of the $Cu-OH_2{}^{2+}$ cation. Considering the macrobicycle L^1, molecular models have shown that the reduced dimension of the macrocyclic cavity does not allow the inclusion of the $Cu-OH_2$ unit.[18] In fact, in the crystal structure of $[CuL^1][ClO_4]_2\cdot0.4MeOH$, the metal ion is co-ordinated by the four nitrogens and completes its co-ordination environment by binding an oxygen of the trioxa chain (Fig. 1).

Again, the $[CuL^1][ClO_4]_2$ complex shows almost the same electronic spectra in both aqueous solution (λ_{max} = 585 nm, ε = 400 dm^3 mol^{-1} cm^{-1}) and in the solid state (λ_{max} = 585 nm), suggesting that the co-ordination features shown by the crystal structure of $[CuL^1]^{2+}$ ion are also maintained in solution.

Zn^{2+} *and* Cd^{2+} *Co-ordination.* The Zn^{2+} and Cd^{2+} ions form $[ML^1]^{2+}$ and $[ML^2]^{2+}$ species characterized by formation constants somewhat lower with respect to the corresponding Cu^{2+} complexes. However, it is noteworthy that such a difference in stability is not as large as usually reported for tetraazacycloalkanes.[16] For example, in the case of the monocycle 1,4,8,11-tetramethyl-1,4,8,11-tetraazacyclotetradecane (L′), characterized by all tertiary nitrogens, the formation constants for the $[CuL']^{2+}$ and $[ZnL']^{2+}$ complexes are respectively 18.3 and 10.35 (in logarithmic units).[19] This can be explained taking into account that the co-ordination properties of these compounds are strongly influenced by the molecular topology.

In order to obtain further information on the co-ordination features of the Zn^{2+} and Cd^{2+} complexes ^{13}C and ^1H NMR spectra at various pH values have been recorded, and, for the case of the system $Zn^{2+}-L^1$, the ^1H spectra are reported in Fig. 3. The ^{13}C NMR spectrum of the ligand at pH 12, where the unprotonated form predominates in solution shows six slightly broad peaks at δ 44.1 (C^3), 51.3 (C^1), 54.5 (C^2), 56.6 (C^4), 68.4 (C^5) and 70.2 (C^6 and C^7). The corresponding ^1H NMR signals are much broader, most likely due to the formation of slowly interchanging (on the NMR time-scale) conformers. However, by using $^1H-^1H$ homonuclear and $^1H-^{13}C$ heteronuclear correlation, the ^1H signals can be assigned and the results are reported in Fig. 3(*a*).

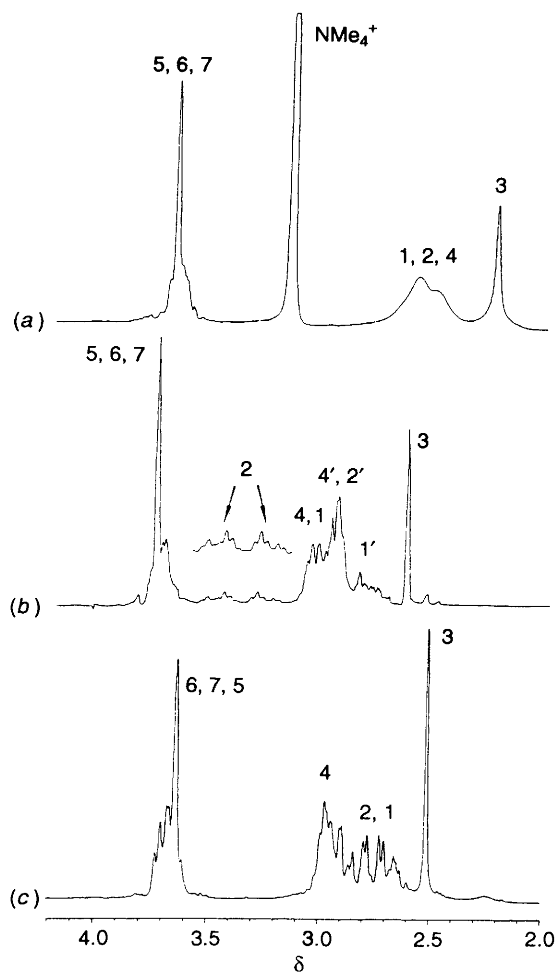

Fig. 3 ^1H NMR spectra of L^1 at pH 12.8 (*a*), $[ZnL^1]^{2+}$ (pH 6.5) (*b*) and $[ZnL^1(OH)_2]$ (pH 10.5) (*c*)

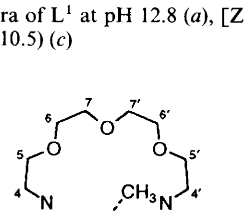

The ^1H and ^{13}C NMR spectra of the Zn^{2+} complex, recorded at pH 6.5, where the $[ZnL^1]^{2+}$ species prevails in solution (see Fig. 4), are in accord with a C_2 time-averaged symmetry. With respect to the spectrum of the free ligand, the resonances of the hydrogen atoms of the carbons adjacent to the amino groups exhibit a remarkable downfield shift, as shown in Fig. 3(*b*). On the other hand, the signals of the hydrogens of the polyoxa chain [with the exception of C(4)] do not shift appreciably. These spectral characteristics suggest that the Zn^{2+} ion is co-ordinated by the tetraaza moity of the macrobicycles, while the trioxa chain does not interact with the metal ions.

The ^1H [Fig. 3(*c*)] and ^{13}C NMR spectra recorded at pH 10.5 differ remarkably from those of the $[ZnL^1]^{2+}$ species. The ^{13}C spectrum displays seven sharp peaks at 45.4 (C^3), 51.5 (C^1), 54.1 (C^2), 56.3 (C^4), 66.9 (C^5), 70.1 (C^6) and 70.9 (C^7), in accord with a C_{2v} symmetry averaged on the NMR time-scale. Such different features between the spectra at pH 6.5 and 10.5 can be explained by taking into account the formation of a $[ZnL^1(OH)_2]$ species, as shown by the potentiometric measurements. For the remaining Cd–L and Zn–L systems (L = L^1 or L^2), similar NMR results seem to indicate that the

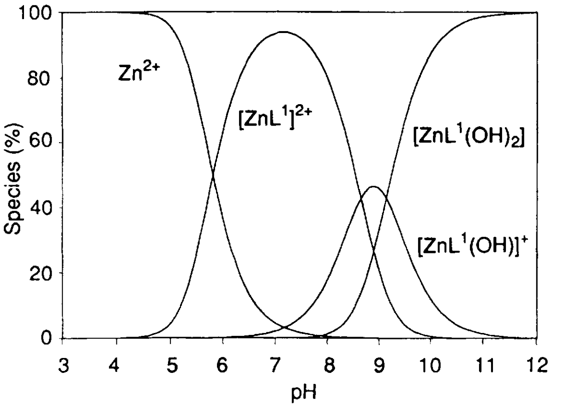

Fig. 4 Species distribution diagram as a function of pH for the system Zn^{2+}–L^1 in 0.15 mol dm^{-3} NMe_4ClO_4 solution at 318.1 K; $[L^1] = 1 \times 10^{-3}$ mol dm^{-3}

oxygens of the bridging chain do not bind to the metal centre in aqueous solution.

It is extremely difficult to rationalize the co-ordination geometry and the stability of the Zn^{2+} and Cd^{2+} complexes. However, both the Zn–L and Cd–L systems give rise to $[ZnL(OH)_2]$ and $[CdL(OH)_2]$ species in aqueous solution. Such behaviour, together with the NMR results, could suggest that two water molecules are bound to the metal ions in the $[ZnL]^{2+}$ and $[CdL]^{2+}$ complexes. In other words, the metal ion would be co-ordinated by the four nitrogen donors and two water molecules from the medium. Taking into account that interaction of the complexed metal with solvent through the N_4 basal plane seems to be hindered by the ethylenic chains of the tetraaza moiety (see Figs. 1 and 2), we can suggest for such complexes the structure shown in Fig. 5. Hydrogen bonds between the water molecule and the oxygens of the macrobicyclic framework could stabilize such species.

Co-ordination of alkali-metal ions.—The binding characteristics of both L^1 and L^2 towards alkali-metal ions have been also analysed in 0.15 mol dm^{-3} NMe_4ClO_4 at 298.1 K. The ligand L^1 can bind the Na^+ ion [log $K = 2.2(1)$],* while it does not interact with Li^+ and K^+, at least under the pH range investigated (3–11). On the contrary L^2 co-ordinates the Li^+ ion [log $K = 2.5(1)$] but does not bind the Na^+ and K^+ ions. Such values are in accord with the encapsulation of the alkali cations into the three-dimensional cavity of the ligands.[1a,c] Furthermore, the ^7Li NMR spectrum of $[LiL^2]^+$ in aqueous solution is characterized by one sharp resonance at δ 0.75. By addition of LiCl a second sharp signal due to the solvated Li^+ ion appears in the spectrum, indicating a slow exchange between the co-ordinated metal ion and the free Li^+ ion, on the NMR time-scale. These features are usually due to the inclusion of the cation into the macrobicyclic cavity.[20] The Li^+–Na^+ selectivity exhibited by these cryptands is rather surprising, considering that the cryptand L^2 is characterized by a larger cavity with respect to L^1. These binding features can result from the balance between both the dimension and form of the three-dimensional cavity and the number, type and disposition of the donor atoms.

Dissociation Kinetics.—The kinetics of dissociation of the Cu^{2+} complexes of L^1 and L^2 has been studied at different temperatures in 1 mol dm^{-3} $HClO_4$ and the results are reported in Table 4. For both complexes the rates of dissociation are first order in the complex concentration.

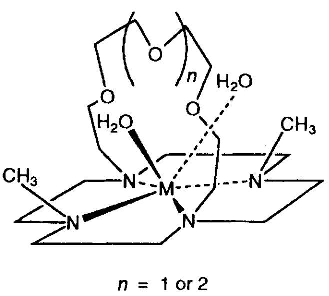

Fig. 5 Proposed structure for the $[ML(H_2O)_2]^{2+}$ complexes (M = Zn, Cd) in aqueous solution

Table 4 Rate constants and activation parameters for dissociation of the Cu^{2+} complexes with L^1 and L^2 in 1 mol dm^{-3} $HClO_4$

	T/K	10^6k/ min^{-1}	$E_a{}^a$/kJ mol^{-1}	$\Delta H^‡$/kJ mol^{-1}	$\Delta G^‡$/kJ mol^{-1}	$\Delta S^‡$/J mol^{-1} K^{-1}
L^1	298	$0.12(1)^{a,b}$	80(2)	77(2)	112.5(4)	−114(10)
	317	0.835(2)				
	324	1.88(1)				
	327	2.25(5)				
	331	2.85(8)				
L^2	298	$0.41(1)^b$	74(2)	71(2)	109.4(4)	−127(10)
	317	2.58(3)				
	324	4.6(1)				
	327	5.7(1)				
	331	8.2(1)				

[a] Obtained by least-square fitting of the rate constants determined experimentally at different temperatures ($\ln k = A - E_a/RT$). [b] Values in parentheses are standard deviations on the last significant figure.

A generally accepted mechanism for the acidic dissociation of Cu^{2+} complexes with tetraazacycloalkanes[21] involves in the rate-determining step the detachment and protonation of a co-ordinated nitrogen atom. This process would be completed by the association of water molecules to the Cu^{2+} ion. As a consequence, second-order rate constants are usually found in the acidic dissociation of polyazamacrocyclic complexes. However, in the present case, the H^+ concentration can be reasonably considered constant ([L] = 0.005 mol dm^{-3}) explaining the observed first-order rate constants.

Considering the activation free energy $\Delta G^‡$, detachment and protonation of a bound nitrogen to allow a water molecule to co-ordinate to the vacant site of the metal centre is indeed an unfavourable step, and is usually characterized by largely positive enthalpic contributions to the activation process. In the present case, it is of interest that the dissociation reaction is far slower than those reported for tetraazacycloalkanes. In particular, the $\Delta H^‡$ contribution to the activation process is much higher than that observed for most monocyclic polyammino complexes.[21] Indeed, the molecular crowding and stiffening due to the presence of both methyl groups and polyoxa bridging chains can hinder the rearrangement of the tetraazamacrocyclic framework required for protonation and detachment of a nitrogen atom, therefore explaining the largely unfavourable $\Delta H^‡$ terms. In this context, the higher $\Delta H^‡$ values found for $[CuL^1]^{2+}$ with respect to $[CuL^2]^{2+}$ can be explained by taking into account the larger bridging chain presented by the latter ligand. However, such a difference in the enthalpic contribution to the activation process could be also ascribed to the different co-ordination environments presented by the two complexes.

It is noteworthy that the Cu^{2+} complexes of the receptors L^3 and L^4 which present the same tetraaza moiety with respect to L^1 and L^2 do not dissociate, even on heating in strong acidic media. This behaviour has been explained by considering that the metal ion is tightly encapsulated inside the rigid macrobicyclic framework.[20] However, such ligands are

---

* These formation constants are relative to the equilibrium $L + M^+ \rightleftharpoons [ML]^+$, where $M = Li^+$ or Na^+ and $L = L^1$ or L^2. The values in parentheses are standard deviations on the last significant figure.

characterized by a remarkably shorter bridging chain and consequently by a more rigid backbone with respect to both L^1 and L^2. These features confirm the basic role played by molecular hindrance and rigidity in determining the rate of dissociation of this kind of complex.

Experimental

Synthesis.—The macrocycles L^1 and L^2 and their salts $[H_2L^1][ClO_4]_2\cdot H_2O$ and $[H_2L^2][ClO_4]_2\cdot H_2O$ were obtained as reported in ref. 10. Both ligands had satisfactory elemental analyses.

$[CuL^1][ClO_4]_2\cdot 0.4MeOH$. A solution of $Cu(ClO_4)_2\cdot 6H_2O$ (37.1 mg, 0.1 mmol) in water (5 cm^3) was slowly added to a boiling solution (5 cm^3) of L^1 (35.8 mg, 0.01 mmol) in methanol. The resulting solution was refluxed for *ca.* 30 min. Blue crystals of the complex suitable for X-ray analysis were obtained by slow evaporation at room temperature of this solution. Yield: 45 mg (72%) (Found: C, 34.8; H, 6.2; N, 8.8. Calc. for $C_{18.4}H_{39.6}Cl_2CuN_4O_{11.4}$: C, 34.85; H, 6.30; N, 8.85%).

CAUTION: Perchlorate salts of metal complexes with organic ligands are potentially explosive; these compounds must be handled with great care.

$[CuL^2][ClO_4]_2$. A solution of $Cu(ClO_4)_2\cdot 6H_2O$ (37.1 mg, 0.1 mmol) in methanol (5 cm^3) was added to a boiling solution of L^2 (40.2 mg, 0.1 mmol) in methanol (10 cm^3). The resulting solution was refluxed for *ca.* 30 min. After cooling to room temperature, butanol was added until the formation of a violet precipitate occurred. The complex was filtered off under nitrogen, washed with methanol–butanol (1:1) and dried *in vacuo*. Yield: 38 mg (57%) (Found: C, 36.2; H, 6.4; N, 8.5. Calc. for $C_{20}H_{42}Cl_2CuN_4O_{12}$: C, 36.10; H, 6.35; N, 8.40%).

$[CuL^2(H_2O)][ClO_4]_2$. A solution of $Cu(ClO_4)_2\cdot 6H_2O$ (37.1 mg, 0.1 mmol) in water (5 cm^3) was slowly added to a boiling solution of L^2 (40.2 mg, 0.1 mmol) in water (15 cm^3). The resulting solution was refluxed for *ca.* 40 min. By slow evaporation blue crystals of the complex, suitable for X-ray analysis were obtained. Yield: 43 mg (63%) (Found: C, 35.3; H, 6.5; N, 8.2. Calc. for $C_{20}H_{44}Cl_2CuN_4O_{13}$: C, 35.15; H, 6.50; N, 8.20%).

This complex can also be obtained in quantitative yield by exposing $[CuL^2][ClO_4]_2$ to the air at room temperature; on the contrary, $[CuL^2][ClO_4]_2$ can be synthesized in quantitative yield by heating $[CuL^2(H_2O)][ClO_4]_2$ at 80 °C for a few minutes (see Discussion section).

Structure Determination.—*Crystal data*. $[CuL^1][ClO_4]_2\cdot 0.4MeOH$, $C_{18.4}H_{39.6}Cl_2CuN_4O_{11.4}$, M = 633.79, monoclinic, a = 10.054(4), b = 16.400(5), c = 16.532(4) Å, β = 92.66(2)°, U = 2723(2) Å^3 (by least-squares refinement on diffractometer setting angles for 25 automatically centred reflections, λ = 0.710 69 Å), space group $P2_1$, Z = 4, D_c = 1.55 g cm^{-3}, $F(000)$ = 1328.8. Air-sensitive prismatic blue crystals (approximate dimensions 0.3 × 0.4 × 0.4 mm), μ(Mo-Kα) = 10.60 cm^{-1}.

$[CuL^2(H_2O)][ClO_4]_2$, $C_{20}H_{44}Cl_2CuN_4O_{13}$, M = 683.04, monoclinic, a = 10.646(2), b = 11.088(8), c = 12.654(3) Å, β = 92.22(2)°, U = 1474(1) Å^3 (by least-squares refinement on diffractometer setting angles for 25 automatically centred reflections, λ = 0.710 69 Å), space group $P2_1$, Z = 2, D_c = 1.54 g cm^{-3}, $F(000)$ = 718. Prismatic blue crystals (approximate dimensions 0.5 × 0.3 × 0.2 mm), μ(Mo-Kα) = 9.89 cm^{-1}.

Data collection and processing.[22] $[CuL^1][ClO_4]_2\cdot 0.4MeOH$: CAD4 X-ray diffractometer, θ–2θ scan mode with θ scan width

Table 5 Positional parameters (× 10^4) with estimated standard deviations in parentheses, for $[CuL^1][ClO_4]_2\cdot 0.4MeOH$

Atom	*x*	*y*	*z*
Cu(1)	−2 093(4)	0	−27(2)
Cu(2)	−7 988(4)	−1 285(3)	−4 575(2)
Cl(1)	−2 616(10)	231(8)	−3 791(5)
Cl(2)	−1 428(11)	−3 040(8)	−7 342(6)
Cl(3)	−2 547(11)	−3 475(8)	−2 805(6)
Cl(4)	−7 394(10)	−1 512(7)	−431(7)
O(11)	−1 483(37)	−29(28)	−3 400(20)
O(21)	−3 260(42)	−454(27)	−4 162(24)
O(31)	−2 350(40)	626(28)	−4 531(25)
O(41)	−3 523(36)	566(24)	−3 327(21)
O(12)	−1 485(34)	−2 977(23)	−6 475(20)
O(22)	−1 789(39)	−3 799(29)	−7 642(22)
O(32)	−7 754(61)	2 563(43)	−2 330(35)
O(42)	−338(40)	−2 647(26)	−7 714(22)
O(13)	−2 386(27)	−3 277(19)	−3 617(17)
O(23)	−2 032(56)	−2 840(39)	−2 298(32)
O(33)	−3 204(82)	−4 082(59)	−2 769(50)
O(43)	−3 813(61)	−3 007(42)	−2 591(34)
O(14)	−8 396(38)	−2 024(25)	−638(21)
O(24)	−6 130(72)	−1 756(44)	−628(37)
O(34)	−7 392(64)	−931(42)	−1 121(37)
O(44)	−7 654(41)	−1 221(33)	320(26)
N(1)	−1 057(27)	716(19)	−782(16)
C(1)	−899(32)	255(20)	−1 576(17)
C(2)	−985(33)	−660(21)	−1 419(19)
N(2)	−2 283(26)	−840(18)	−1 009(15)
C(3)	−3 511(40)	−708(29)	−1 522(24)
C(4)	−2 182(33)	−1 659(21)	−633(17)
C(5)	−1 779(48)	−1 598(31)	286(25)
N(3)	−2 288(22)	−956(14)	700(12)
C(6)	−1 502(39)	−812(27)	1 476(23)
C(7)	−246(40)	−238(25)	1 261(24)
N(4)	−915(30)	542(20)	902(17)
C(8)	−1 394(38)	1 098(25)	1 520(21)
C(9)	202(30)	1 038(21)	527(17)
C(10)	287(34)	720(24)	−320(19)
C(11)	−1 567(39)	1 565(27)	−918(24)
C(12)	−2 982(40)	1 550(30)	−1 312(25)
O(1)	−3 786(22)	1 133(15)	−928(12)
C(13)	−5 137(47)	1 254(36)	−1 323(30)
C(14)	−5 988(56)	1 003(36)	−826(31)
O(2)	−6 395(24)	1 432(16)	−168(15)
C(15)	−6 131(45)	1 245(34)	498(27)
C(16)	−4 717(43)	1 031(30)	849(26)
O(3)	−4 143(24)	221(16)	593(13)
C(17)	−4 354(36)	−360(22)	1 209(20)
C(18)	−3 613(29)	−1 089(20)	927(17)
N(5)	−7 358(26)	−1 254(22)	−3 405(14)
C(19)	−7 416(43)	−412(26)	−3 200(23)
C(20)	−6 926(38)	142(27)	−3 489(19)
N(6)	−7 247(27)	−20(21)	−4 616(15)
C(21)	−6 310(29)	47(24)	−5 200(16)
C(22)	−8 663(34)	374(24)	−4 877(19)
C(23)	−9 172(50)	−7(35)	−5 603(25)
N(7)	−9 453(36)	−963(23)	−5 487(21)
C(24)	−10 641(35)	−1 081(23)	−4 944(19)
C(25)	−10 494(37)	−1 939(24)	−4 717(22)
N(8)	−9 316(27)	−2 095(18)	−4 221(15)
C(26)	−8 870(40)	−2 950(27)	−4 241(23)
C(27)	−9 401(35)	−1 899(23)	−3 370(19)
C(28)	−8 085(51)	−1 917(35)	−3 018(33)
C(29)	−5 911(43)	−1 529(30)	−3 303(25)
C(30)	−5 550(41)	−2 098(27)	−3 796(22)
O(4)	−6 100(24)	−2 012(16)	−4 623(14)
C(31)	−5 662(48)	−2 679(34)	−5 285(28)
C(32)	−4 330(42)	−2 315(29)	−5 575(25)
O(5)	−4 589(33)	−1 684(22)	−6 129(19)
C(33)	−5 133(54)	−1 923(35)	−6 834(29)
C(34)	−6 126(47)	−1 447(35)	−7 132(27)
O(6)	−7 216(36)	−1 497(25)	−6 545(20)
C(35)	−8 604(45)	−1 256(39)	−6 958(27)
C(36)	−9 615(36)	−1 302(30)	−6 279(20)
C(40)	−6 616(47)	−4 755(30)	−3 495(26)
O(41)	−7 125(42)	−5 478(28)	−3 291(23)

0.70 + 0.35 tan θ°, θ scan rate variable, graphite-monochromated Mo-Kα radiation, T ambient; Lorentz, polarization and intensity decay corrections applied (observed intensity decay at the end of data collection was 54.2% with respect to the initial intensity); 4753 reflections measured (2θ range 5–40°, ± h, k, l), 2006 unique observed reflections [$I > 3.0\sigma(I)$].

$[CuL^2(H_2O)][ClO_4]_2$: CAD4 diffractometer, θ–2θ scan mode with θ scan width 0.85 + 0.35 tan θ°, θ scan rate variable, graphite-monochromated Mo-Kα radiation, T ambient; Lorentz and polarization corrections applied; 2856 reflections measured (2θ range 5–50°, ± h, k, l), 2004 unique observed reflections [$I > 3.0\sigma(I)$].

Structure analysis and refinement. $[CuL^1][ClO_4]_2\cdot0.4MeOH$: Patterson method and subsequent Fourier syntheses. Full-matrix least-squares refinements. Two independent molecules found in the elemental cell. Absorption correction after structure resolution (DIFABS[22]); the decrease in R due to the application of the absorption correction is < 1%. Copper and chlorine atoms anisotropic, hydrogen atoms in calculated positions with overall, fixed thermal parameters (U = 0.05 Å^2). The carbon, oxygen and hydrogen atoms of a disordered methanol molecule refined with 0.8 occupancy. 326 Refined parameters; R = 0.1034 and R' = 0.1031 [$w = a/\sigma^2(F) + 0.0015F^2$, where a is an adjustable parameter]; with the other enantiomorph the corresponding values are R = 0.1037 and R' = 0.1035. The high values for R and R' were the result of decomposition of the crystal, the disordered solvent molecule and the presence of four perchlorate anions. Consequently the absolute configuration of the crystal could not be determined unequivocally. The atomic coordinates are given in Table 5.

$[CuL^2(H_2O)][ClO_4]_2$: Patterson method and subsequent Fourier syntheses. Full-matrix least-squares refinements. Absorption correction after structure resolution (DIFABS); the decrease in R due to the application of the absorption correction is < 1%. Copper, chlorine, oxygen and nitrogen atoms anisotropic, hydrogen atoms in calculated positions with overall, fixed thermal parameters (U = 0.05 Å^2). Hydrogen atoms of the water molecule not found in the ΔF map. 260 Refined parameters; R = 0.063, R' = 0.056 [$w = a/\sigma^2(F)$]; the corresponding values for the other enantiomorph are R = 0.064, R' = 0.057. The atomic coordinates are given in Table 6.

Programs and sources of scattering factor data are given in ref. 22. The computer used was a DEX 486-DX.

Additional material available from the Cambridge Crystallographic Data Centre comprises H-atom coordinates, thermal parameters and remaining bond lengths and angles.

E.m.f. Measurements.—The potentiometric measurements were carried out in 0.15 mol dm^{-3} NMe_4ClO_4 by using the equipment described previously.[23] In the case of Cu^{2+}, Zn^{2+} and Cd^{2+} the complex formation reactions with L^1 and L^2 are too slow at 298.1 K to be studied confidently at this temperature and consequently the potentiometric measurements were performed at 318.1 ± 0.1 K. Moreover, the protonation constants for both ligands were redetermined at this temperature. The reference electrode was an Ag–AgCl electrode in saturated KCl solution. The glass electrode was calibrated as a hydrogen concentration probe by titrating known amounts of HCl with CO_2-free NaOH solutions and determining the equivalent point by Gran's method[24] which allows the determination of the standard potential E°, and the ionic product of water (pK_w = 13.83 ± 0.02 at 318.1 K, pK_w = 13.10 ± 0.02 at 298.1 K). At least three titrations were performed for each system, in the pH range 3–10. For Na^+ and Li^+ 100 data points were collected for each titration curve. In the case of Cu^{2+}, Zn^{2+} and Cd^{2+}, due to the slowness of the complexation reactions, the e.m.f. readings were made 40 min after each addition of titrant. 20 Data points were collected for each titration curve. The computer program SUPERQUAD[25] was used to calculate both the protonation and stability constants from the e.m.f. data. The titration curves for each system were treated either as a single set or as separate entities without significant variations in the values of the stability constants.

Table 6 Positional parameters (× 10^4) with estimated standard deviations in parentheses, for $[CuL^2(H_2O)][ClO_4]_2$

Atom	x	y	z
Cu	7 474(1)	5 000	7 984(1)
Cl(1)	7 346(3)	−240(3)	1 493(2)
O(11)	8 346(10)	−83(16)	9 926(9)
O(12)	6 258(10)	−614(11)	9 757(8)
O(13)	7 137(12)	856(10)	10 968(10)
O(14)	7 684(17)	−1 131(13)	11 235(11)
Cl(2)	9 202(4)	5 262(4)	3 297(3)
O(21)	9 344(13)	4 102(12)	3 771(12)
O(22)	9 559(15)	6 144(14)	4 121(10)
O(23)	7 954(13)	5 438(13)	2 877(11)
O(24)	9 909(14)	5 348(16)	2 500(9)
O(5)	5 739(7)	5 311(8)	6 991(6)
N(1)	7 343(10)	3 265(9)	8 554(7)
C(1)	8 044(14)	3 445(12)	9 657(11)
C(2)	7 436(14)	4 428(12)	10 178(11)
N(2)	7 373(9)	5 539(8)	9 506(7)
C(20)	6 286(13)	6 274(13)	9 676(11)
C(3)	8 540(12)	6 247(12)	9 777(10)
C(4)	8 641(11)	7 198(11)	8 917(9)
N(3)	8 534(9)	6 594(9)	7 870(8)
C(5)	9 722(12)	6 038(13)	7 718(10)
C(6)	9 488(12)	5 177(15)	6 748(9)
N(4)	8 515(10)	4 296(11)	6 898(8)
C(40)	7 784(15)	3 946(16)	5 857(11)
C(7)	9 104(15)	3 247(15)	7 478(13)
C(8)	8 101(15)	2 516(14)	7 937(12)
C(9)	6 091(13)	2 725(13)	8 631(10)
C(10)	5 292(18)	2 296(19)	7 731(13)
O(1)	5 197(10)	2 770(9)	6 765(7)
C(11)	4 100(13)	2 411(14)	6 047(11)
C(12)	3 110(16)	3 348(15)	5 951(14)
O(2)	3 555(8)	4 423(9)	5 553(7)
C(13)	2 621(15)	5 419(15)	5 318(11)
C(14)	2 617(14)	6 269(14)	6 097(12)
O(3)	3 699(8)	7 013(9)	6 205(8)
C(15)	3 804(15)	7 816(14)	7 095(12)
C(16)	4 912(14)	8 533(14)	7 071(13)
O(4)	5 956(8)	7 771(8)	7 211(8)
C(17)	7 064(14)	8 369(14)	7 106(12)
C(18)	8 101(12)	7 458(12)	6 967(10)

NMR Spectroscopy.—200.0 MHz ^1H and 50.32 MHz ^{13}C NMR spectra in D_2O solutions at different pH values were recorded at 318 K in a Bruker AC-200 spectrometer. In the ^1H NMR spectra the peak positions are reported relative to HOD at δ 4.75. Dioxane was used as the standard reference in the ^{13}C NMR spectra (δ 67.4). Small amounts of NMe_4OH or HCl were added to the solutions to adjust the pD. The pH was calculated from the measured pD values using the relationship:[26] pH = pD − 0.40. Lithium-7 NMR spectra were recorded at an operating frequency of 77.78 MHz. Peak positions are reported relative to a 10^{-3} mol dm^{-3} LiCl aqueous solution (δ 0).

Electronic Spectroscopy.—The electronic spectra were recorded on a Perkin-Elmer Lambda 9 spectrophotometer equipped with a 1 cm cell thermostatted at 298 K.

Kinetic Measurements.—Solutions containing known amounts of $[CuL^1]^{2+}$ and $[CuL^2]^{2+}$ (complex concentration 0.005 mol dm^{-3} in both cases) in pure water were prepared from $[H_2L^1][ClO_4]_2\cdot H_2O$ or $[H_2L^2(H_2O)][ClO_4]_2$, Cu^{2+} stock solution and the calculated volume of standardised NaOH solution, and allowed to equilibrate at 298 K. Solutions of the complexes in 1 mol dm^{-3} $HClO_4$ were prepared by mixing the previous solutions with the appropriate quantities of concentrated standardised acid. All the acidic solutions were stored in a thermostat. The experiments were conducted at 317, 324, 327 and 331 K. Portions of these solutions were taken from the thermostat, cooled rapidly to room temperature and placed in the spectrophotometer, thermostatted at 298 K, in a 1 cm quartz cell. The dissociation of both complexes at 298 K is very slow, as shown by preliminary measurements, thus allowing handling of the acidic solutions of the complexes at this temperature. The kinetics of dissociation was followed by monitoring the absorbance at 585 nm in the case of L^1 and at 625 nm in the case of L^2. First-order plots of the data were linear for at least four half-lives.

Acknowledgements

Financial support by Italian Ministero dell'Università e della Ricerca Scientifica e Tecnologica (quota 60%) and Progetto Finalizzato di Chimica Fine e Secondaria of the Italian Research Council (CNR) is gratefully acknowledged.

References

1 (*a*) R. M. Izatt, J. S. Bradshaw, S. A. Nielsen, J. D. Lamb, J. J. Christensen and D. Sen, *Chem. Rev.*, 1985, **85**, 271; (*b*) K. E. Krakowiak, J. S. Bradshaw and D. J. Zamecka-Krakowiak, *Chem. Rev.*, 1989, **89**, 929; (*c*) R. M. Izatt, K. Pawlak, J. S. Bradshaw and R. L. Bruening, *Chem. Rev.*, 1991, **91**, 1721; (*d*) J. S. Bradshaw, K. E. Krakowiak and R. M. Izatt, *Tetrahedron*, 1992, **48**, 4475; (*e*) J. M. Lehn, *Angew. Chem., Int. Ed. Engl.*, 1988, **27**, 89; (*f*) *Synthesis of Macrocycles, the Design of Selective Complexing Agents*, eds. J. J. Christensen and R. M. Izatt, Wiley, New York, 1987; (*g*) K. B. Mertes and J. M. Lehn, in *Comprehensive Coordination Chemistry*, ed. G. Wilkinson, Pergamon Press, Oxford, 1987, p. 915; (*h*) G. W. Gokel, *Crown Ethers and Cryptands*, Monographs in Supramolecular Chemistry, ed. J. F. Stoddart, The Royal Society of Chemistry, Cambridge, 1992.

2 *The Chemistry of Macrocyclic Ligand Complexes*, ed. L. F. Lindoy, Cambridge University Press, Cambridge, 1989; M. Dobler, *Ionophores and their Structure*, Wiley Interscience, New York, 1981.

3 C. Pascard, C. Riche, M. Cesario, F. Kotzyba-Hibert and J. M. Lehn, *J. Chem. Soc., Chem. Commun.*, 1982, 557; A. Kumar, S. Mageswaran and I. O. Sutherland, *Tetrahedron*, 1986, **42**, 3291; A. Pratt, I. O. Sutherland and R. F. Newton, *J. Chem. Soc., Perkin Trans. 1*, 1988, 13; I. O. Sutherland, *Chem. Soc. Rev.*, 1986, **15**, 63; I. O. Sutherland, *Pure Appl. Chem.*, 1989, **61**, 1547.

4 E. Graf, J. P. Kintzinger, J. M. Lehn and J. Le Moigne, *J. Am. Chem. Soc.*, 1982, **104**, 1672.

5 B. Metz, J. M. Rosalky and R. Weiss, *J. Chem. Soc., Chem. Commun.*, 1976, 533.

6 J. M. Lehn, *Acc. Chem. Res.*, 1978, 49.

7 J. M. Lehn, *Pure Appl. Chem.*, 1978, **50**, 871.

8 B. Diederich, M. W. Hosseini, J. M. Lehn and R. B. Session, *J. Am. Chem. Soc.*, 1981, **103**, 1282; M. W. Hosseini, J. M. Lehn and M. P. Mertes, *Helv. Chim. Acta*, 1983, **66**, 2454; M. W. Hosseini, J. M. Lehn, L. Maggiora, M. P. Mertes and K. B. Mertes, *J. Am. Chem. Soc.*, 1985, **107**, 909; M. W. Hosseini, J. M. Lehn, L. Maggiora, M. P. Mertes and K. B. Mertes, *J. Am. Chem. Soc.*, 1987, **109**, 537; M. W. Hosseini and J. M. Lehn, *Helv. Chim. Acta*, 1988, **71**, 749; M. P. Mertes and K. B. Mertes, *Acc. Chem. Res.*, 1990, **23**, 413 and refs. therein.

9 F. Vögtle, H. Sieger and M. W. Müller, *Top. Curr. Chem.*, 1981, **98**, 107; R. M. Izatt, K. Pawlak, J. S. Bradshaw, R. L. Bruening and B. J. Tarbet, *Chem. Rev.*, 1992, **92**, 1261.

10 C. Bazzicalupi, A. Bencini, A. Bianchi, V. Fusi, P. Paoletti and B. Valtancoli, *J. Chem. Soc., Perkin Trans. 2*, 1994, 815.

11 C. K. Johnson, ORTEP, Report ORNL-3794, Oak Ridge National Laboratory, Oak Ridge, TN, 1971.

12 P. O. Anderson and A. B. Packand, *Inorg. Chem.*, 1979, **18**, 7; J. W. L. Martin, P. R. Rudolf, J. H. Timmons, A. E. Martell and A. Clearfield, *Inorg. Chem.*, 1981, **20**, 814; B. J. Hathaway and D. E. Billing, *Coord. Chem. Rev.*, 1970, **5**, 143.

13 K. A. Beveridge, A. McAuley and C. Xu, *Inorg. Chem.*, 1991, **30**, 2074.

14 M. Ciampolini, M. Micheloni, F. Vizza, F. Zanobini, S. Chimichi and P. Dapporto, *J. Chem. Soc., Dalton Trans.*, 1986, 505.

15 A. Bencini, A. Bianchi, P. Dapporto, V. Fusi, E. Garcia-España, M. Micheloni, P. Paoletti, P. Paoli, A. Ridriguez and B. Valtancoli, *Inorg. Chem.*, 1993, **32**, 2753.

16 A. Bianchi, M. Micheloni and P. Paoletti, *Coord. Chem. Rev.*, 1991, **110**, 17; A. Bencini, A. Bianchi, P. Paoletti and P. Paoli, *Coord. Chem. Rev.*, 1992, **120**, 51.

17 C. Bazzicalupi, A. Bencini, A. Bianchi, V. Fusi, E. Garcia-España, P. Paoletti, P. Paoli and B. Valtancoli, *Inorg. Chem.*, 1993, **32**, 4900; A. Andres, C. Bazzicalupi, A. Bencini, A. Bianchi, V. Fusi, E. Garcia-España, P. Paoletti, P. Paoli and B. Valtancoli, *Inorg. Chem.*, 1994, **33**, 617.

18 HyperChem, AUTODESK inc., Sausaliti, CA, 1992.

19 B. S. Nakani, J. J. B. Welsh and R. D. Hancock, *Inorg. Chem.*, 1983, **22**, 2956; B. S. Nakani and R. D. Hancock, *S. Afr. J. Chem.*, 1983, **36**, 117.

20 M. Ciampolini, N. Nardi, B. Valtancoli and M. Micheloni, *Coord. Chem. Rev.*, 1992, **120**, 223; A. Bencini, A. Bianchi, A. Borselli, S. Chimichi, M. Ciampolini, E. Garcia-España, P. Dapporto, M. Micheloni, P. Paoli and B. Valtancoli, *Inorg. Chem.*, 1989, **28**, 4279; A. Bianchi, M. Ciampolini, M. Micheloni, N. Nardi, B. Valtancoli, S. Mangani, E. Garcia-Espãna and J. A. Ramirez, *J. Chem. Soc., Perkin Trans. 2*, 1989, 1131.

21 D. K. Cabbiness and D. W. Margerum, *J. Am. Chem. Soc.*, 1970, **92**, 2151; R. W. Renfrew, R. S. Jamison and D. C. Wheaterburn, *Inorg. Chem.*, 1979, **18**, 1584; R. W. Hay, R. Bembi, W. T. Moodie and P. R. Norrhan, *J. Chem. Soc., Dalton Trans.*, 1982, 2131; R. W. Hay, R. Bembi, F. McLaren and W. T. Moodie, *Inorg. Chim. Acta*, 1984, 23.

22 G. M. Sheldrick, SHELX-76, Program for Crystal Structure Determination, University of Cambridge, 1976; DIFABS, N. Walker and D. D. Stuart, *Acta Crystallogr., Sect. A*, 1983, **39**, 158; *International Tables for X-Ray Crystallography*, Kynoch Press, Birmingham, 1974, vol. 4.

23 A. Bianchi, L. Bologni, P. Dapporto, M. Micheloni and P. Paoletti, *Inorg. Chem.*, 1984, **23**, 1201.

24 G. Gran, *Analyst (London)*, 1952, **77**, 661; F. J. Rossotti and H. Rossotti, *J. Chem. Educ.*, 1965, **42**, 375.

25 P. Gans, A. Sabatini and A. Vacca, *J. Chem. Soc., Dalton Trans.*, 1985, 1195.

26 A. K. Covington, M. Paabo, R. A. Robinson and R. G. Bates, *Anal. Chem.*, 1968, **40**, 700.

Received 7th June 1994; *Paper* 4/03421J